American Society of Mechanical Engineers

ASME Accepted Manuscript Repository

Institutional Repository Cover Sheet

Cranfield Collection of E-Research - CERES

ASME Paper Title: Boeing 737-400 passenger air conditioner control system model for accurate fault simulation

Authors: Shafayat H. Chowdhury, Fakhre Ali, Ian K. Jennions

ASME Journal Title: Journal of Thermal Science and Engineering Applications

Volume/Issue: Volume 14, Issue 9 Date of Publication (VOR* Online) 2 February 2022

ASME Digital Collection URL: https://asmedigitalcollection.asme.org/thermalscienceapplication/article/14/9/091008/1134927/Boeing-737-400-Passenger-Air-Conditioner-Control

DOI: https://doi.org/10.1115/1.4053740

*VOR (version of record)

Journal of Thermal Science and Engineering Applications.
Received September 17, 2021;Accepted manuscript posted January 25, 2022.
doi:10.1115/1.4053740
Copyright © 2022 by ASME

Final Manuscript: TSEA-21-1530

Boeing 737-400 Passenger Air Conditioner Control System Model for Accurate Fault Simulation

Shafayat H. Chowdhury[1], Fakhre Ali, Ian K. Jennions
IVHM Centre, Cranfield University, Bedfordshire, MK430AL, United Kingdom

Abstract

The aircraft environmental control system (ECS) is a highly integrated and complex system. The passenger air conditioner (PACK) is the heart of the ECS and has been reported as a key driver of unscheduled maintenance by aircraft operators. This is principally due to the PACK's ability to compensate for degraded components, and hence mask their real condition, so that when failure occurs it is a major event. The development of an accurate diagnostic solution would identify the degradation early and hence focus effective maintenance and reduce cost. This paper is a continuation of the authors' work on the development of a systematically derived PACK simulation for accurate fault diagnostics, utilising a model-based approach. In practise the PACK simulation accuracy is dependent on a number of factors, which include the understanding of its control system. This paper addresses this by taking an in-depth look at the factors controlling the operation of the PACK in order to enable the gap between the theoretical understanding of the PACK and the engineering design of the system to be bridged, and accurate simulations under healthy and degraded scenarios obtained. The paper provides a comprehensive explanation of the PACK control system elements (principally valves) and verifies their operation based on experimental test data acquired from a B737-400 aircraft. A discussion of the control used in the simulation is then given, resulting in the correct temperature, pressure and flow being delivered to the cabin. The overall simulation results are then presented to demonstrate the importance of employing a systematically derived control logic. They are then further used to assess the impact of degradation in the main PACK valves.

Accepted Manuscript Not Copyedited

[1] Corresponding author.
E-mail address: shafayat.chowdhury@cranfield.ac.uk (Shafayat Hasan Chowdhury)

Published by The American Society of Mechanical Engineers. This is the Author Accepted Manuscript issued with:
Creative Commons Attribution License (CC BY). The final published version is available online at DOI:10.1115/1.4053740.
Please refer to any applicable publisher terms of use.

Journal of Thermal Science and Engineering Applications. Received September 17, 2021;
Accepted manuscript posted January 25, 2022. doi:10.1115/1.4053740
Copyright © 2022 by ASME

Nomenclature

Acronyms

Alt	Altitude (m)
ACM	Air Cycle Machine
ADS	Air Distribution System
APU	Auxiliary Power Unit
B737	Boeing 737
CHX	Condenser
DS	Degradation Severity[%]
ECS	Environmental Control System
HPWS	High Pressure Water Separator
PACK	Passenger Air Conditioner
PO	PACK Outlet
PV	PACK Valve
PVIP	PACK Valve Inlet Pressure[kPa]
PVOP	PACK Valve Outlet Pressure [kPa]
PHX	Primary Heat Exchanger
RAM	RAM- ambient air
RC	Reference Case
RH	Relative Humidity [%]
RHX	Reheater
SESAC	Simscape ECS Simulation under All Conditions
SHX	Secondary Heat Exchanger
TCV	Temperature Control Valve
WS	Water Separator

Subscript

C_{PR}	Compressor pressure ratio
CMP_i	Compressor inlet
CMP_o	Compressor outlet
$CHX_{h,i}$	Condenser hot inlet
$CHX_{h,o}$	Condenser hot outlet
$CHX_{c,i}$	Condenser cold inlet
$CHX_{c,o}$	Condenser cold outlet
P	Pressure (kPa)
P_{BAS}	Bleed air pressure (kPa)
P_{Cab}	Cabin Pressure (kPa)
P_{vi}	PACK valve inlet
P_{vo}	PACK valve outlet
PV_θ	PACK Valve Angle[°]
$PHX_{h,i}$	Primary heat exchanger hot inlet
$PHX_{h,i}$	Primary heat exchanger hot outlet
P_{amb}	Ambient Pressure (kPa)
PCK_o	PACK outlet
$RHX_{h,i}$	Reheater hot inlet
$RHX_{h,o}$	Reheater hot outlet
$RHX_{c,i}$	Reheater cold inlet
$RHX_{c,o}$	Reheater cold outlet
$SHX_{h,i}$	Secondary heat exchanger hot inlet

Accepted Manuscript Not Copyedited

Journal of Thermal Science and Engineering Applications. Received September 17, 2021;
Accepted manuscript posted January 25, 2022. doi:10.1115/1.4053740
Copyright © 2022 by ASME

$SHX_{h,o}$	Secondary heat exchanger hot outlet
T_{amb}	Ambient Temperature (K)
T_{ci}	Cold side inlet temperature (K)
TRB_i	Turbine inlet
TRB_o	Turbine inlet
T_{co}	Cold side outlet temperature (K)
T_{PR}	Turbine pressure ratio
T_{BAS}	Bleed air temperature (K)
T_{Cab}	Cabin temperature (K)
WS_o	Water separator Outlet

Greek Symbols

$\dot{m}$	Mass flow (kg/s)
$\dot{m}_c$	Cold mass flow (kg/s)
$\dot{m}_{target}$	Cabin mass flow (kg/s)
T_{target}	Target Temperature[K]
ϵ	Effectiveness (%)

Accepted Manuscript Not Copyedited

Journal of Thermal Science and Engineering Applications. Received September 17, 2021;
Accepted manuscript posted January 25, 2022. doi:10.1115/1.4053740
Copyright © 2022 by ASME

1 Introduction

All commercial aircraft are equipped with an air conditioning system, commonly known as the Environmental Control System (ECS). The ECS is responsible for two key functions: (i) providing pressurised air to the anti-icing system, and: (ii) regulating cabin temperature (T), pressure (P) and humidity. The heart of the ECS is the Passenger Air Conditioner (PACK), whose components are prone to degradation, with operators reporting the PACK to be one of the key drivers of unscheduled maintenance. The overall functionality of the PACK is dependent on the synergistic operation of various sub-systems - heat exchangers, valves, a compressor and a turbine - making it a complicated system with maintenance problems that may not have a clear root cause. Recent studies of the ECS have reported strong interdependencies between the sub-systems of the PACK, specifically when subjected to degradation [1, 2]. Furthermore, the PACK control system focusses the performance characteristics of the PACK sub-systems on set targets, and therefore has the potential to mask degradation in its components [1]. For these reasons the determination of accurate control logic is vital for capturing the physics of the system operating in healthy and faulty scenarios.

There is a compelling requirement from industry to identify innovative retrofit Condition Based Maintenance (CBM) solutions for supporting a robust maintenance strategy on legacy aircraft [3]. Model-based approaches for diagnosis have been predominantly used and purposed for CBM implementation, due to their intuitive engineering approach. This includes identification of sensor set optimisation, followed by calculation of the difference between sensor data and model data to isolate fault occurrences at sub-system level [4-6]. A simulation model that can accurately capture the physics and engineering of the PACK at sub-system level, under a wide range of functional scenarios, is required, both to focus maintenance activities and reduce cost. In collaboration with Boeing, the IVHM Centre at Cranfield University is conducting research on the ECS and has developed an ECS simulation model: Simscape ECS Simulation under all Conditions (SESAC) [7]. Based on the successful implementation of SESAC, the performance evaluation of the PACK under healthy, and some degraded, operating scenarios have been studied by the current authors [1].

The thermodynamic performance characteristics of the PACK sub-systems such as the RAM heat exchangers, the bleed flow control valve, the Temperature Control Valve (TCV) as well as the Air-Cycle Machine (ACM) are found to be strongly influenced by the control logic employed within the simulation model, especially when components are exposed to degradation. In order to implement accurate control over the PACK it is necessary to understand not only the objective goals of the system but also the detailed operation of some of the sub-systems, i.e. valves, thus providing the focus for this paper.

1.1 Scope of Work

Previous papers in this project have detailed the construction of an ECS simulation code (SESAC), capable of replicating healthy flight conditions and some cases of component degradation [1, 7]. In practise this simulation is only as good as the understanding of the control system allows, and the availability of experimental data for validation. This paper addresses the first of these, taking an in-depth look at the factors controlling the operation of the PACK in order to have the highest possible confidence in the validity of the simulations, specifically when simulating degradation at sub-system level.

Accepted Manuscript Not Copyedited

Journal of Thermal Science and Engineering Applications. Received September 17, 2021;
Accepted manuscript posted January 25, 2022. doi:10.1115/1.4053740
Copyright © 2022 by ASME

In order to understand the PACK control system, it has proved necessary to understand the engineering of the overall control logic and some of the PACK elements, to enable the gap between the theoretical understanding of the PACK and the original design of the system to be bridged. For the aircraft under study, the Boeing 737-400 (B737-400), the PACK control logic is composed of the following elements:

- Operation of the PACK bleed flow control valve, known as the PACK Valve (PV)
- A built-in overheat protection system
- Operation of the temperature control valves (TCV)
- Control over the RAM air that provides cold air to the heat exchangers

All these topics are appropriately addressed in this paper. The paper provides a comprehensive explanation of the PACK control system elements and verifies their operation based on experimental test data acquired from the B737-400 aircraft. PACK simulation results are presented to substantiate the importance of employing systematically derived control logic to enable accurate fault simulation. Finally, simulations are conducted to assess the degradation in control system elements, i.e. PV and TCV.

1.2 Overview of the ECS and PACK Functionality

The ECS is powered by bleed air supplied by the main engines or the APU. The PACK, a schematic of which is shown in Figure 1, is the core of the ECS; it conditions the bleed air depending on aircraft cabin demand. Following the PACK, the Air Distribution System (ADS) filters and distributes the conditioned air to the flight deck, passenger cabin and avionics bay. There are normally two PACKs in most narrow and wide-body civil aircraft, both PACKs are generally installed in parallel on either side of the aircraft centreline, on the underside of the fuselage.

Following the sequence of the flow and station numbers shown in Figure 1, the PACK PV_i receives bleed air at high temperature and pressure, primary cooling takes place in the PHX, and secondary cooling takes place in the SHX, the flow is subsequently compressor in the compressor (CMP_o). Cold RAM air labelled as PHX_{ci} and SHX_{ci}, which originates from outside the aircraft, flows through the RAM air duct and, after being used as a heat sink for PHX and SHX, is deposited back into the aircraft's airstream. After the SHX the temperature of the bleed air has been substantially reduced and is passed through a series of heat exchangers within the HPWS in order to treat the air for humidity. Subsequent to that, the high pressure flow is expanded through a turbine. At the outlet of the turbine (TRB_o) the air temperature can potentially drop below freezing and, if this occurs, it is addressed by mixing part of the bypass hot bleed flow through the TCV-Pri_o. The mixing of this air is controlled in order to match the PACK outlet temperature against the cabin demand, this temperature is generally referred to as the target temperature (T_{target}).

The PV and TCV in the PACK regulate the hot mass flow through the system and the core in order to sufficiently support the overall functionality of the PACK. This requires a number of control logic paths in order to regulate the valve positions which will be investigated in this paper.

Accepted Manuscript Not Copyedited

Journal of Thermal Science and Engineering Applications. Received September 17, 2021;
Accepted manuscript posted January 25, 2022. doi:10.1115/1.4053740
Copyright © 2022 by ASME

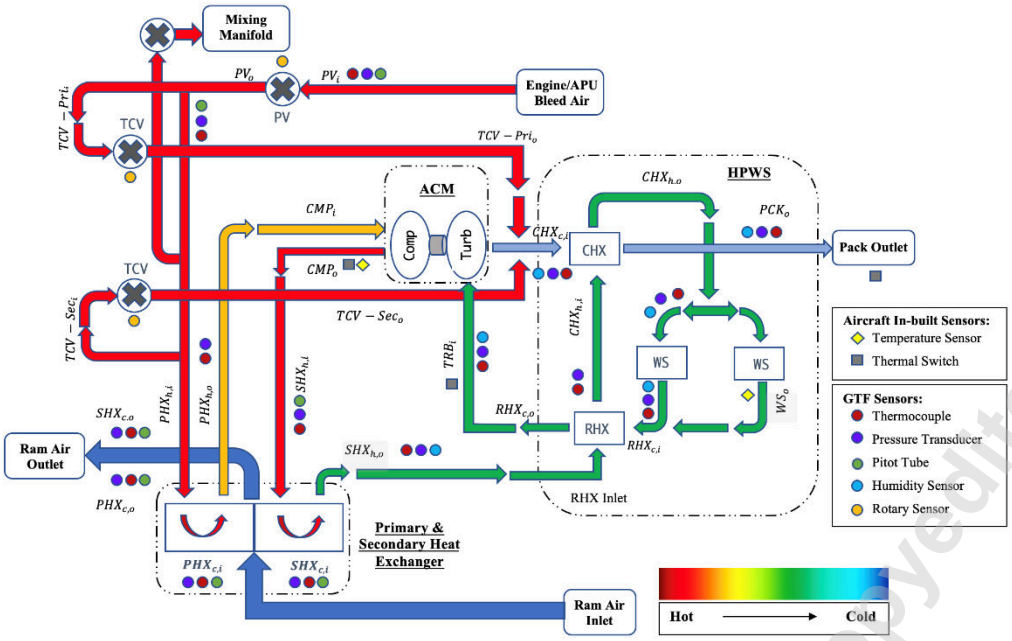


Figure 1: Component level schematic of the B737 PACK with the labelling of the airflow sequence.

1.3 PACK Simulation Framework - SESAC

SESAC is a simulation framework that offers the implementation of an object-oriented modelling approach, enabling a drag-and-drop interface, where each component of the ECS is independently formulated. This approach allows the flexibility to integrate components together to represent an overall ECS system, allowing the acquisition of system performance parameters at each component's inlet and outlet. Furthermore, SESAC provides component sub-libraries, e.g. a dedicated library is assigned to represent healthy and faulty components, and the ability to input component design characteristic maps.

SESAC is capable of simulating the performance characteristics of the ECS under a wide range of operating conditions and functional scenarios. Fault severities can be introduced to each component, and multiple faults can be simulated simultaneously. The theoretical and computational development of SESAC has been previously reported by the authors [7].

1.4 Boeing 737 Ground Test Facility

A full scale Boeing 737-400 aircraft ground test facility has been developed at Cranfield University. The aircraft major sub-systems, such as the ECS and APU, have been instrumented with various types of condition monitoring sensors [8]. These sensors allow the acquisition of system health state parameters at sub-system level.

The left-side PACK of Cranfield's B737, as shown in Figure 2, has been instrumented with sensors in order to measure pressure, temperature, mass flow (P, T, $\dot{m}$) and humidity (not discussed here) throughout the PACK, located as shown in Figure 1. The aim of this experimental work is to support validation of SESAC and, in a step towards this, to support the verification of the PACK control system used in the simulation. The adopted scenarios used here represent: (i) a fault free, healthy run and: (ii) a faulty run, having an abrupt PACK shutdown due to a RAM air door failure.

Accepted Manuscript Not Copyedited

Journal of Thermal Science and Engineering Applications. Received September 17, 2021;
Accepted manuscript posted January 25, 2022. doi:10.1115/1.4053740
Copyright © 2022 by ASME

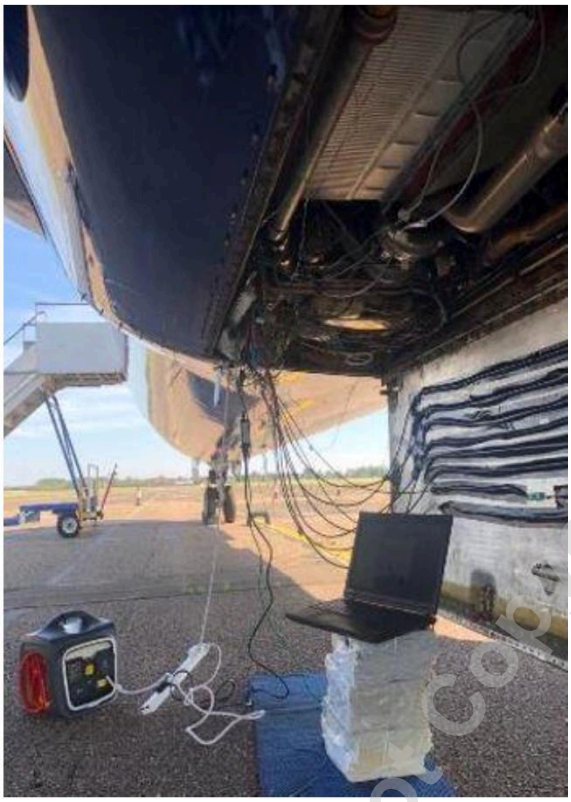


Figure 2: Ground test facility of the Boeing 737-400, Left-side PACK data collection.

2 PACK Control System

The temperature demanded by the aircraft generally ranges between 18℃ and 30℃ [9]. The flight crew set the temperature demand using the temperature controls mounted on the P5 overhead panel in the cockpit. This information is then supplied to the PACK controller, which controls the operation of the PACK accordingly. Figure 3 shows the elements of the control system, comprising:

1. The PV to control the bleed mass flow into the PACK.
2. The in-build thermal switches for PACK overheat protection.
3. The TCV and RAM air flow control to regulate the merge outlet temperature.

Each of these is described below, in this order.

Accepted Manuscript Not Copyedited

Journal of Thermal Science and Engineering Applications. Received September 17, 2021;
Accepted manuscript posted January 25, 2022. doi:10.1115/1.4053740
Copyright © 2022 by ASME

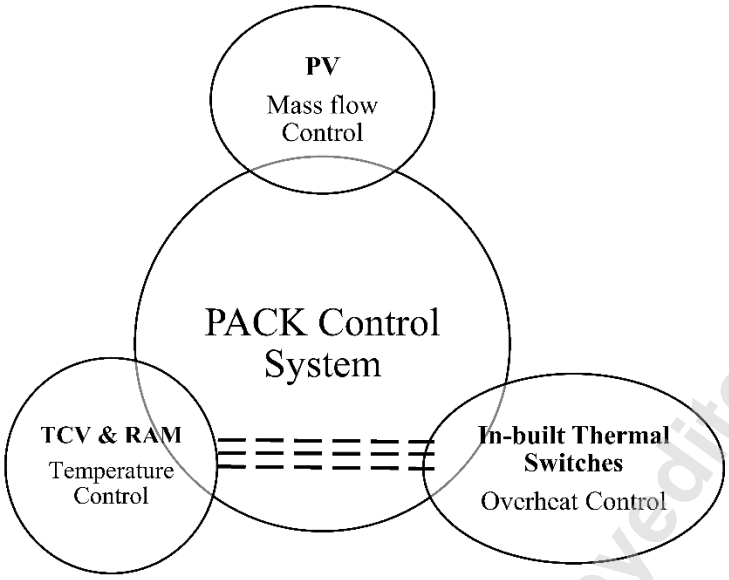


Figure 3: Overall elements of the PACK control system: overheat protection, temperature control and mass flow control.

2.1 Mass Flow Control System

The PV is a butterfly valve with a venturi, a set of solenoids and air chambers, servo valve, total pressure sensing ports, pressure regulator, control orifice and a valve positioning indicator as shown in Figure 4. It is pneumatically controlled and actuated and responds to a number of inputs to effectively deliver a constant mass flow into the PACK. The servo valves are spring-loaded; opening and closing based on the pressure difference between the upstream, venturi, and downstream pressures. The air pressure in the chambers keeps adjusting until the desired mass flow through the valve is achieved. There are 2 different options available on the P5 overhead panel in the cockpit to run the pack – auto and high setting. While the auto setting is used for nominal operating condition, the high setting is used to power a single PACK in case of the other PACK failing. The high setting is also used on the ground, with single PACK operation, to achieve maximum cooling. As per the AMM [9], the overall PACK operation can be divided into two key operational states: (i) ground operation, and (ii) in-flight operation. During ground operations, since the aircraft main engines are switched off, the on-board auxiliary power unit supplies the bleed flow to the left PACK only, which represents the maximum flow scenario compared to the in-flight scenarios. During in-flight conditions, the main engines provide the required bleed flow. In case of any in-flight PACK failure, the single PACK operation is maintained under high mass flow settings in order to maintain required cabin pressurisation and temperature. Under normal in-flight operation both PACK work in unison to supply the demanded cabin conditions. A qualitative view of this is presented in Fig. 4.

Accepted Manuscript Not Copyedited

Journal of Thermal Science and Engineering Applications. Received September 17, 2021;
Accepted manuscript posted January 25, 2022. doi:10.1115/1.4053740
Copyright © 2022 by ASME

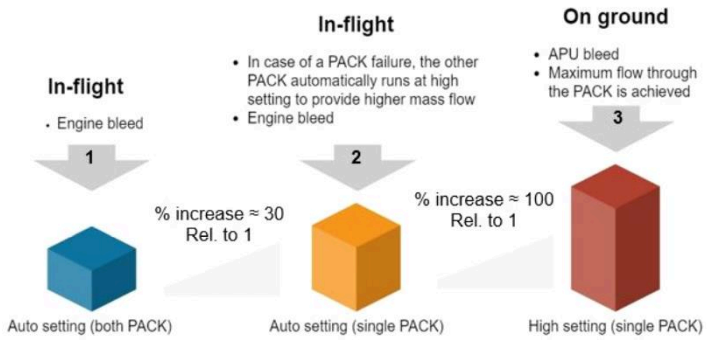


Figure 4: Illustration of the various PACK operational scenarios and their corresponding relative magnitude of mass flow.

The PV starts operating as the open-close solenoid *C,* shown in Figure 5, is energised retracting the ball valve actuator allowing controlled air flow through the control orifice to the actuator. This airflow is supplied by the upstream sense port. As the pressure in chamber *A* increases the actuator opens the butterfly valve and allows bleed air into the PACK. As mass flow through the valve increases the velocity of the airflow in the venturi and the upstream pressure increases. This results in pressure drop at chamber *B* and increase in pressure at chamber *C* and *D*. As the differential pressure in between chamber *B* and *C* increases the spring-loaded servo valve opens releasing pressure from chamber *A*. This moves the valve towards its closed position. This increase and decrease in pressure at chamber A continues until the valve reaches steady-state [9].

Accepted Manuscript Not Copyedited

Journal of Thermal Science and Engineering Applications. Received September 17, 2021;
Accepted manuscript posted January 25, 2022. doi:10.1115/1.4053740
Copyright © 2022 by ASME

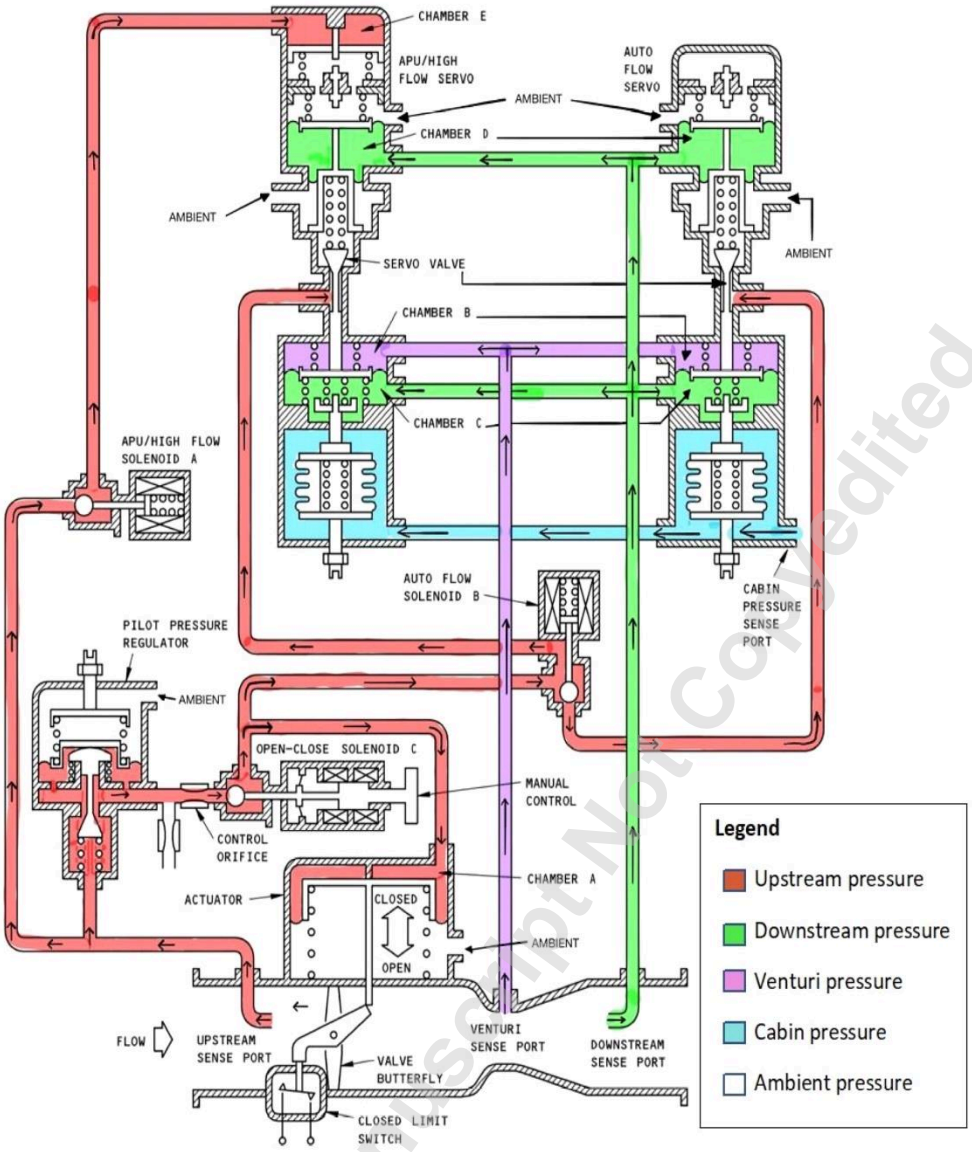


Figure 5: Schematic of the PV, adopted and reproduced from Boeing 737-400 AMM [7].

2.2 Overheat Protection

The PACK can experience overheat for a number of reasons. Generally, the PACK overheat can be caused due to: (i) malfunction of a component, e.g. sticking of PV, TCV or of the ram air modulating door, or: (ii) degradation of components, e.g. fouling or blockage of heat exchangers, or due to fouling or mechanical damage of the ACM. An aircraft incident occurred due to PV malfunction on a Boeing 737-700 flight to Melbourne in 2007 [10]. The aircraft experienced a failure of the right hand engine bleed during take-off. The flight was continued with only one PACK operational but, subsequently, during the climb to Flight level 350 (35000ft), the left air conditioning PACK valve malfunctioned. This resulted in the PACK shutting down and an emergency descent followed with passenger oxygen masks deploying as the cabin altitude exceeded 14000 feet.

To ensure the safety of the PACK system, three inbuilt thermal switches have been included in the PACK at different locations, as shown in Table 1. Each switch is prescribed with

Accepted Manuscript Not Copyedited

Journal of Thermal Science and Engineering Applications. Received September 17, 2021;
Accepted manuscript posted January 25, 2022. doi:10.1115/1.4053740
Copyright © 2022 by ASME

a temperature limit which, if exceeded, will activate the corresponding switch and the PACK controller will process the signal to immediately shut down the PACK by closing the PV.

Table 1: Locations of inbuilt thermal switches for overheat protection [9]

Inbuilt Thermal Switch	Location	Activation temperature limit
Compressor outlet overheat switch	Compressor outlet duct (CMP_o)	199 ^oC
Turbine inlet overheat switch	Reheater outlet duct (TRB_i)	99 ^oC
PACK outlet overheat switch	Upstream of the check valve at the PACK outlet (PCK_o)	121 ^oC

The ram air inlet supplies the required cold mass flow for the primary (PHX) and secondary (SHX) cooling of the hot bleed air. In flight, air is readily captured from the aircraft's motion, but on the ground a small turbo-fan is used to force air through the ram duct. In case of the ram air door or turbo-fan malfunctioning the amount of cold mass flow supplied to both the PHX and SHX is significantly influenced. Under these conditions, it has been established from previous studies reported by authors [1] that the increase in the PHX outlet temperature propagates through the compressor and results in an increased compressor outlet temperature, possibly triggering the compressor outlet overheat switch.

Figure 6(a) presents the test data for a healthy PACK run, having the RAM air door open and the turbo-fan running. The temperature readings at compressor outlet, turbine inlet and PACK outlet are shown against the test time. Both PHX and SHX are supplied with the required cold mass flow and therefore the temperatures approach a steady state value and remain below the thermal switch activation thresholds tabulated in Table 1. Figure 6(b) shows the case when the RAM turbo-fan malfunctions and both PHX and SHX receive no cooling flow. Here much hotter than intended air passes through the compressor and results in a dramatic increase in compressor outlet temperature, and activation of the compressor outlet thermal switch at 199 ^oC. In response, the control system immediately shuts the PACK valve in order to prevent overheating.

Accepted Manuscript Not Copyedited

Journal of Thermal Science and Engineering Applications. Received September 17, 2021;
Accepted manuscript posted January 25, 2022. doi:10.1115/1.4053740
Copyright © 2022 by ASME

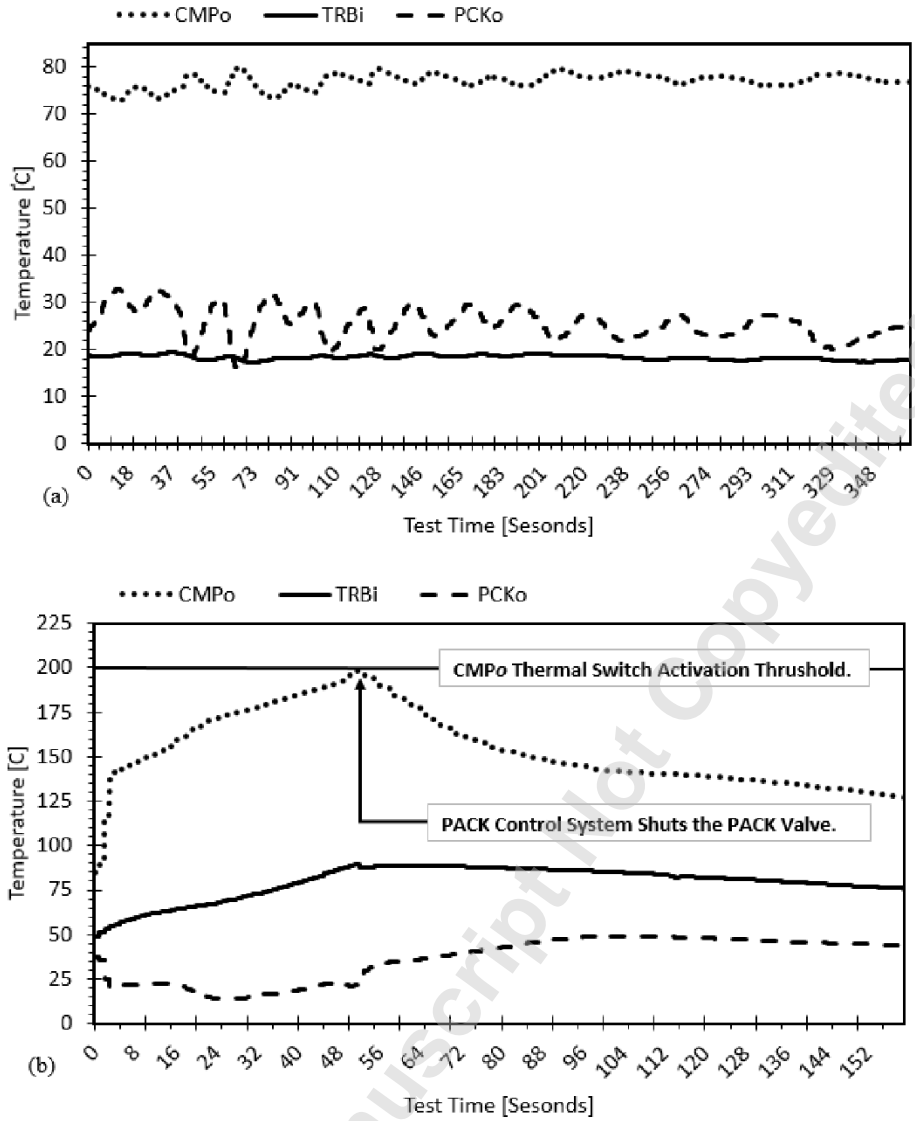


Figure 6: Compressor outlet thermal switch activation (a) data during ground run with the RAM turbofan switched on, (b) data during ground run with the RAM turbofan switched off.

2.3 Temperature Control System

2.3.1 Temperature Control Valve

There are two TCVs in the PACK – a primary temperature control valve and a standby temperature control valve. The primary TCV is electrically controlled and mechanically actuated. The standby TCV is pneumatically and electrically controlled and pneumatically actuated. These valves are controlled through sensing the WS outlet temperature. While both the TCVs regulate the PACK outlet temperature by varying bleed air into the turbine merge, the standby temperature control valve is only used to prevent ice formation at the turbine outlet.

Both the TCVs are butterfly valves. Based on the error between the demand and WS outlet temperature an electric motor drives a shaft rotating the butterfly valve to the desired opening. To enable this the sensor data is processed in the PACK control unit and the output

Accepted Manuscript Not Copyedited

Journal of Thermal Science and Engineering Applications. Received September 17, 2021;
Accepted manuscript posted January 25, 2022. doi:10.1115/1.4053740
Copyright © 2022 by ASME

signal controls the single-phase ac motor to achieve the lowest cabin demand at the PACK outlet. There are other sensors in the mixing manifold, and also inside the cabin, which are used to reach the desired cabin temperatures.

The standby TCV presented in Figure 7 provides two different functions: (i) de-icing and (ii) PACK outlet temperature control (when the primary TCV fails). In contrast to the PV, the stand-by TCV has two parts – pneumatic and electrical. The pneumatic side of the valve works similar to the PV. The chambers in the TCV detect pressure differential across the CHX and based on the valve upstream pressure it uses the pneumatic actuator to change the valve location. This part of the valve is used for de-icing in the condenser. There is also a dedicated chamber which has an electric torque motor and a flapper to isolate the pneumatic system and use ambient vent for opening or closing the valve using the pneumatic actuator.

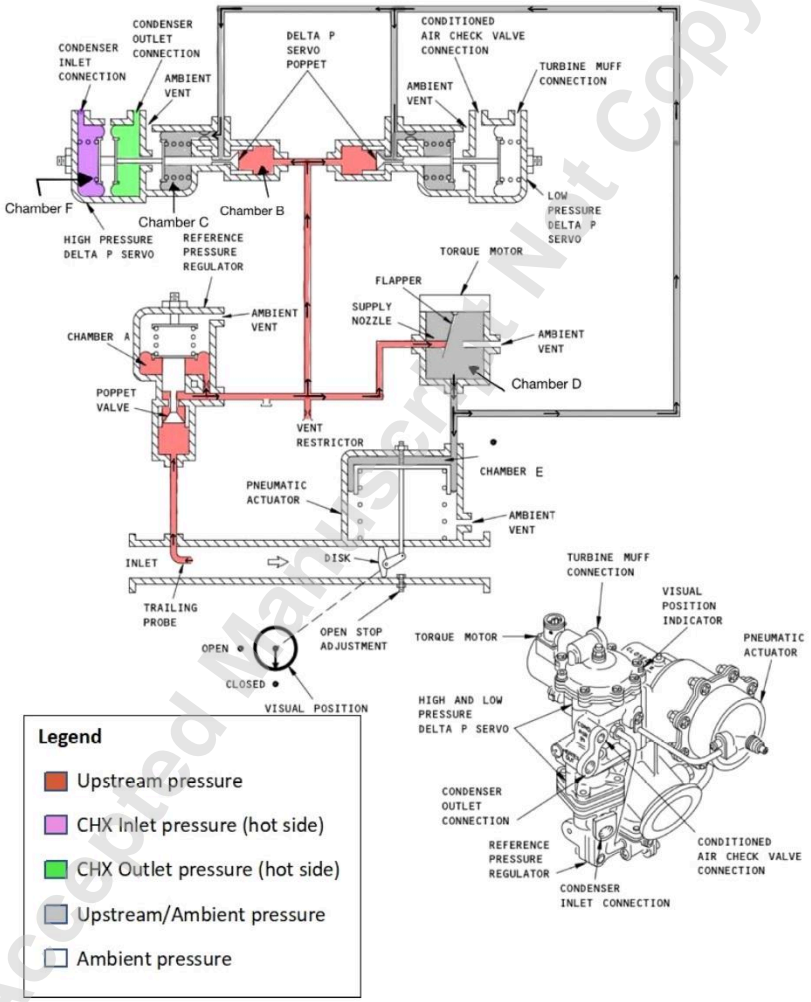


Figure 7: Standby temperature control valve, adopted and reproduced from Boeing 737-400 AMM [7].

Accepted Manuscript Not Copyedited

Journal of Thermal Science and Engineering Applications. Received September 17, 2021;
Accepted manuscript posted January 25, 2022. doi:10.1115/1.4053740
Copyright © 2022 by ASME

2.2.2 Temperature Control Limits

The PACK temperature control primarily acts in two ways: (i) by controlling the cold RAM air supply by regulating the RAM air inlet modulating flap, and: (ii) by controlling the PACK outlet temperature through the hot bypass stream by regulating the TCV, see Figure 1.

It is necessary to regulate the PHX, SHX and turbine outlet temperature to meet the cabin demand using the temperature sensors listed in Table 2. These two inbuilt temperature sensors, at compressor outlet and water separator outlet, support the control system with necessary feedback to control the temperature throughout the PACK, and its compliance against the demanded cabin temperature. For the latter, the lowest temperature demand from the cabin is matched as the PACK outlet.

As previously discussed, during aircraft ground operation a small turbofan pulls in the air through the RAM air inlet. The RAM air inlet is maintained at maximum opening to ensure maximum possible air flow supply to the PHX and SHX.

When the aircraft is operated at altitude with flaps fully retracted, the mass flow that can be achieved through the RAM is dependent on the ambient conditions, as well as the flight Mach number. The PACK controller utilises the temperature sensor installed at the compressor outlet to control the supply of RAM air flow through the PHX and SHX in order to maintain the compressor outlet temperature to as near 110˚C as possible. In cases where this temperature limit exceeds 110˚C, the RAM door fully opens, allowing maximum possible mass flow, under this scenario the RAM door full open light will be on in the cockpit P5 overhead control panel. The overheat protection switch discussed in section 2.2 will be triggered in case the compressor outlet temperature exceeds 199˚C, and under this scenario the control system will shut down the PACK valve to prevent overheating.

Table 2: Inbuilt Temperature sensors for PACK temperature control.

Temperature Sensor	**Location**	**Threshold**
RAM air temperature sensor	Compressor outlet duct (CMP_o)	Regulates RAM mass flow by to maintain the compressor outlet temperature to as near 110 ˚C as possible.
PACK temperature sensor	Water extractor outlet duct (WS_o)	Regulates TCV opening to maintain the lowest temperature demand from the zone.

To regulate the PACK outlet temperature, the TCV is set to mix hot bleed air with the cold air coming out of the turbine. The temperature controller processes the sensor signal from the WS outlet duct, which is then used to open or close the TCV, to match the cabin temperature demand. A healthy ground run experiment, with a cabin temperature demand set at auto settings (which represents around 24 ^{o}C), is shown in Figure 8. Both the WS outlet and the

Accepted Manuscript Not Copyedited

Journal of Thermal Science and Engineering Applications. Received September 17, 2021;
Accepted manuscript posted January 25, 2022. doi:10.1115/1.4053740
Copyright © 2022 by ASME

PACK outlet temperatures approach steady-state at an average of 22^{o}C. Note that the target temperature for the WS outlet is set to maintain the lowest cabin demand at the PACK outlet. As the TCV is working continuously to maintain a constant temperature at the WS outlet by mixing hot air at the merge, the PACK outlet temperature can oscillate, and can be different from the lowest cabin demand. The air distribution system, which includes a mixing manifold, the trim system, and the recirculation system, will then regulate air supply to each cabin zone to match their individual temperature demands.

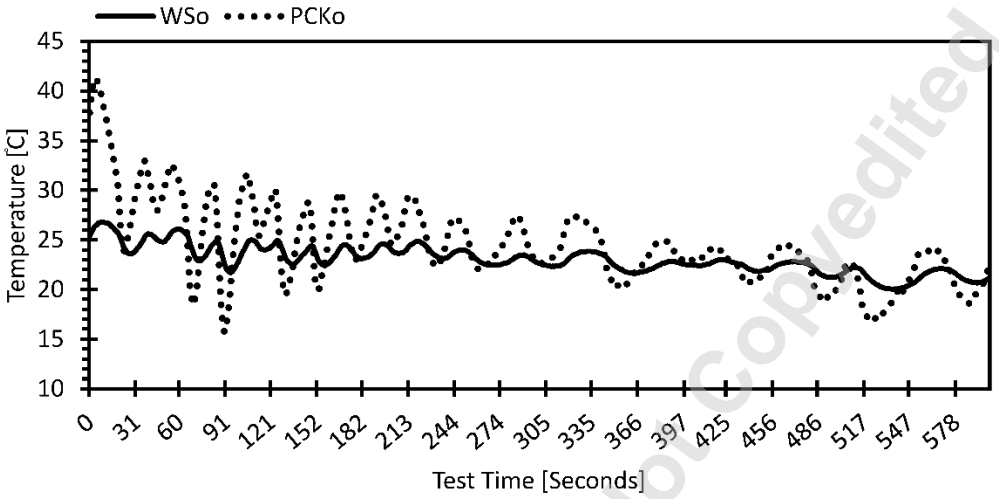


Figure 8: Experimental data, WS outlet and PACK outlet temperature.

3 PACK Simulation Model and Controller

3.1 PACK Simulation Model

Figure 9 presents the B737 PACK model based on the SESAC library. The model configuration in terms of the architecture and flow sequence naturally mirrors the B737 schematic presented in Figure 1. The PACK receives input bleed air at high temperature and pressure from the engine or APU. It conditions this air to meet requirements from the cabin. The addition in Figure 9 is the two feedback loops, one for temperature and one for mass flow. The temperature loop monitors, via a virtual sensor, the merge outlet temperature and controls it by adjusting the amount of hot air admitted to the merge by the TCV. The mass flow loop begins with a virtual sensor at the PACK exit and feeds back to the PACK valve to control the flow against a target value.

The simulation framework SESAC employed within the paper has been verified and validated (V&V) against the actual aircraft data provided by the sponsors at various aircraft cruise points. The overall computational development of the framework and its V&V is reported by the authors in reference [7].

3.2 Boundary Conditions

In order to simulate the performance characteristics of the PACK, under given aircraft operating conditions, boundary conditions for the PACK must be defined. These can be categorised in four parts, as shown in Table 3: (i) Aircraft state condition. This allows the model to determine the RAM mass flow, which serves as the input to the PHX and SHX cold streams. The RAM mass flow is determined based on the aircraft operating conditions, i.e.

Accepted Manuscript Not Copyedited

Journal of Thermal Science and Engineering Applications. Received September 17, 2021;
Accepted manuscript posted January 25, 2022. doi:10.1115/1.4053740
Copyright © 2022 by ASME

Mach number, ambient conditions, and RAM intake geometry. (ii) Bleed air properties, in terms of P, T, specific humidity, and water content are required. (iii) Target outlet conditions, i.e. T, P, and ṁ. (iv) Component health state, represented by the degradation severity (DS) which varies from 0 (healthy) to 100 (fully degraded).

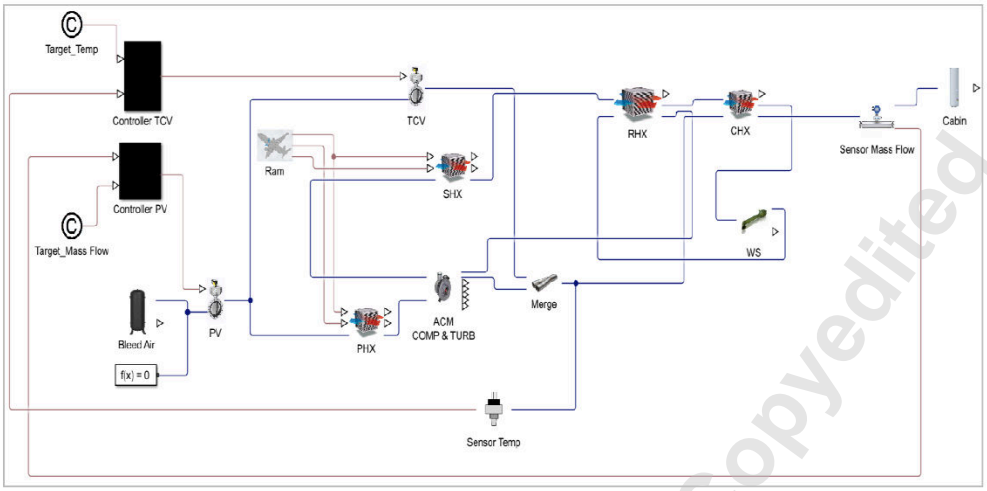


Figure 9: SESAC PACK simulation model for Boeing 737-400, model mirrors the schematic presented in Figure 1.

Table 3: SESAC PACK simulation model boundary conditions.

Component	Parameters	Description	Units
Aircraft State condition	Selector (S)	Determines if the aircraft is in flight or operating at ground static conditions. 1= inflight, 0 = ground static.	[-]
Ram (0: Ground Static)	ṁ	Ram ṁ is required if aircraft operating at ground static.	[-]
	T_{amb}	Ambient temperature	[K]
	Alt	Aircraft Altitude	[m]
Ram (1: In flight)	Mach	Aircraft Mach number	[-]
	Area	Ram door total area	[m^2]
	%Open	Ram door opening in %	[%]
Bleed Air properties	T_{BAS}	Inlet temperature to PV	[K]
	P_{BAS}	Inlet pressure to PV	[Pa]
	SH_{BAS}	Inlet specific humidity at PV	[kg/k]
	CO_{BAS}	Inlet liquid water content at PV	[kg/k]
Target Conditions	P_{target}	Target pressure	[Pa]
	T_{target}	Target temperature	[K]
	$\dot{m}_{target}$	Target mass flow	[kg/s]
Component health state	*DS*	Degradation severity level	[%]

Accepted Manuscript Not Copyedited

Journal of Thermal Science and Engineering Applications. Received September 17, 2021;
Accepted manuscript posted January 25, 2022. doi:10.1115/1.4053740
Copyright © 2022 by ASME

3.3 Controller for the PACK Simulation

The PACK fundamentally achieves the temperature control through the TCV and regulates the mass flow through the pneumatic PV system. To ensure that the target mass flow at the PACK outlet is attained, an appropriate control is required to regulate the PV. Similarly, a separate controller is required for regulating the TCV to achieve the target temperature, as shown in Figure 9. From the Simscape library, the integral controller was selected for the control of the PV and TCV. The schematic of the implemented PV and TCV integral controller are shown in Figure 10. The controller receives a signal from the virtual sensor and calculates the error relative to the target value. A gain is used to amplify the error which is then provided as an input to the integral block. The physical signal (PS) integrator block outputs the integral of its input at the current time step. The integral block requires an initial condition in order to determine the initial state at the beginning of a simulation run (e.g. at time = 0). The following equation represents the output of the integral block for the PV:

$$Y_{(t)} = \int_{t_0}^{t=1} u(t)dt + y_0 \qquad [1]$$

Where, in the case of mass flow control:

u	Amplified mass flow error
Y	Output PV angle
y_0	Initial condition for PV angle
t	Simulation time

Where:

$$Error = \frac{T_{\dot{m}} - Sensor_{\dot{m}}}{T_{\dot{m}}} \qquad [2]$$

The solver computes the output of the integrator block at the current time step, using the current input value and the value of the state at the previous time step. To support this, the integrator block saves its output at the current time step for use by the solver to compute its output at the next time step. Iteratively, the integrator block will continue to perform the computations until the error is zero.

Accepted Manuscript Not Copyedited

Journal of Thermal Science and Engineering Applications. Received September 17, 2021;
Accepted manuscript posted January 25, 2022. doi:10.1115/1.4053740
Copyright © 2022 by ASME

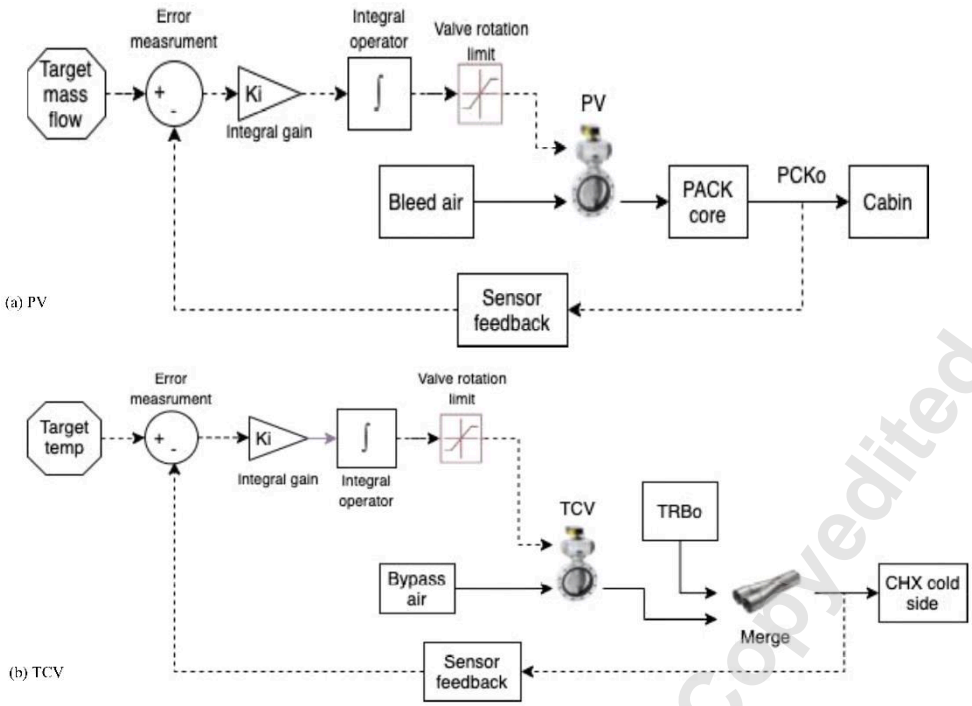


Figure 10: Implemented PS integrator controller for the PV and TCV control in the SESAC PACK model.

Figure 11 presents the response of the integral controller when simulated for healthy and faulty conditions. The faulty condition represents a 50% degradation in the PACK PHX. It can be observed that the response of the controller is robust and time efficient. In both cases, an overshoot can be observed which can be attributed to the initial condition provided to the integrator in terms of the valve angle. For example, in the case of the mass flow, the provided initial condition of the PV angle leads to a higher mass flow than the target, hence the overshoot. The controller therefore reduces the angle through the iterative process in order to match the mass flow. The model presented in Figure 9 with the integral controller for PV and TCV can now be implemented for the assessment of fault simulation of the PACK at component level.

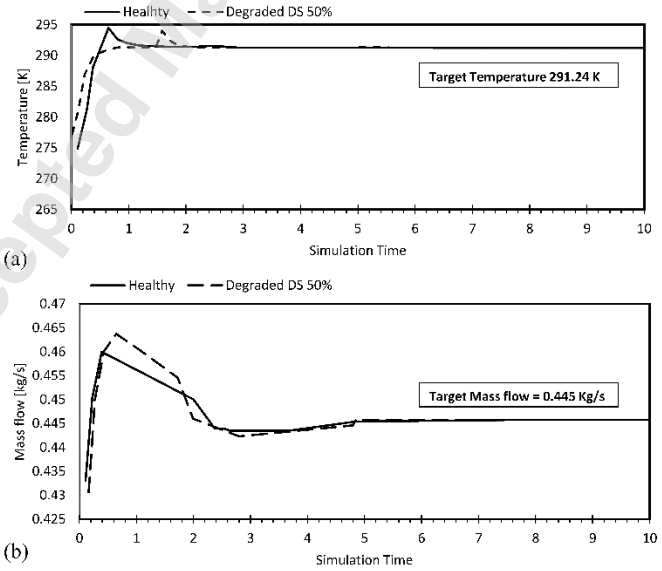


Figure 11: The implemented integral controller response for temperature and mass flow.

Accepted Manuscript Not Copyedited

Journal of Thermal Science and Engineering Applications. Received September 17, 2021;
Accepted manuscript posted January 25, 2022. doi:10.1115/1.4053740
Copyright © 2022 by ASME

4 Results & Discussion

This section is presented in two main parts. In the first part, the PACK performance characteristics in terms of temperature, pressure and mass flow are presented for two reference aircraft cruise operating conditions. Degradation in the PHX is simulated under both conditions, this is done with the view to assess the robustness of the model under varying boundary conditions, and to substantiate the importance of employing systematically derived control logic to enable accurate fault simulation. In the second part, model simulations are conducted to simulate malfunction in the PV and TCV, and their impact on the PACK performance characteristics is discussed.

4.1 Integral controller based PACK fault simulation

Table 4 presents the two reference cruise operating points considered for the demonstration of the PACK fault simulation. The developed SESAC simulation model presented in Figure 9 was implemented to simulate the degradation in the PHX at various degradation severity levels for both references cases. The PACK boundary conditions for both reference cases were provided by the project industrial partner. In Table 4 the inlet, and the outlet target boundary conditions are provided in terms of the PACK inlet pressure, PACK outlet mass flow and the temperature (i.e. target mass flow and temperature). During cruise, the bleed air is extracted from the main engines high pressure compressor, and generally multiple bleed extraction stations are included in order to extract bleed flow at different levels of pressure. It can be observed from Table 4 that, as the aircraft altitude increases from 30000ft to 3500ft between RC1 and RC2. The higher RC2 altitude, having lower outside temperature relative to RC1, considering the heat balance over the aircraft, the cabin temperature demand will rise, therefore demanding relatively cooler flow. To allow the PACK to deliver cooler air flow, the bleed pressure (PVIP) is increased so that the air is supplied to the PACK at higher pressure to allow higher expansion through the ACM turbine.

Table 4: Reference cases implemented for fault simulation.

Reference Case	Altitude	PVIP	$\dot{m}_{target}$ [kg/s]	T_{target} [K]
1	30000 ft	191 kPa	0.4434	295.54
2	35000 ft	230 kPa	0.4234	284.42

4.1.1 RC1 PHX Degradation

Figure 12 presents the simulation results under PHX degradation for RC1. For the degradation of the PHX, the blockage in the PHX cold side intake is considered. The sticking of relatively large dust particles, debris and/or random foreign objects (e.g. a bird), ingested from outside the aircraft through the RAM air intake, cause heat exchanger degradation due to blockage. This flow is not filtered before it is supplied to the PHX, and therefore there is a risk of large dust particles or foreign objects passing through the RAM air intake.

Blockage in the PHX cold side inlet will cause a drop in PHX effectiveness. To simulate the blockage, the PHX effectiveness value acquired under healthy conditions was gradually

Accepted Manuscript Not Copyedited

Journal of Thermal Science and Engineering Applications. Received September 17, 2021;
Accepted manuscript posted January 25, 2022. doi:10.1115/1.4053740
Copyright © 2022 by ASME

degraded (at 10% intervals) in order to simulate various severity levels (e.g. a 10% degradation translates to 10% reduction in the PHX healthy effectiveness value). The reduction in the PHX effectiveness consequently reduces the heat transfer through the PHX and increases its outlet temperature as presented in Figure 12(a). The PHX and SHX are identical units in terms of their design, size, and shape. The large temperature difference at PHX outlet is carried through the compressor unchanged and then the SHX removes most of the excess heat, its outlet temperature only changing slightly. Effectively the PHX and SHX are acting together as one large heat exchanger (Figure 1), both using the RAM air to cool the main flow. They each receive 50% of the RAM air but the SHX can use it more efficiently than the degraded PHX. The entire temperature deficit is not recovered due to the cold RAM flow to the SHX being limited. This results in the overall effect of the PHX fouling on the turbine outlet temperature being minimal.

Due to the increased temperature at the merge, the TCV gradually shuts to allow more mass flow through the turbine in order to achieve maximum expansion and cooling efficiency. The closure of the TCV creates a back pressure on the PV outlet, creating a reduction in pressure across the PV (Figure 12b). As the pressure differential across the valve decreases, the mass flow drops. With increasing level of degradation, the mass flow controller opens the PV, as shown in Figure 13, in order to attempt to match the target mass flow. Until the point where the PV is fully open and cannot deliver any more flow. At this point, under further degradation, the PACK inlet mass flow decreases in order to satisfy the merge conditions, given the PV cannot open any more. The PV saturates at 90% degradation, which corresponds to the maximum back pressure on PV, as the PVOP approaches PVIP (Figure 13), resulting in a marginal drop in PV inlet mass flow (Figure 13c).

Accepted Manuscript Not Copyedited

Journal of Thermal Science and Engineering Applications. Received September 17, 2021;
Accepted manuscript posted January 25, 2022. doi:10.1115/1.4053740
Copyright © 2022 by ASME

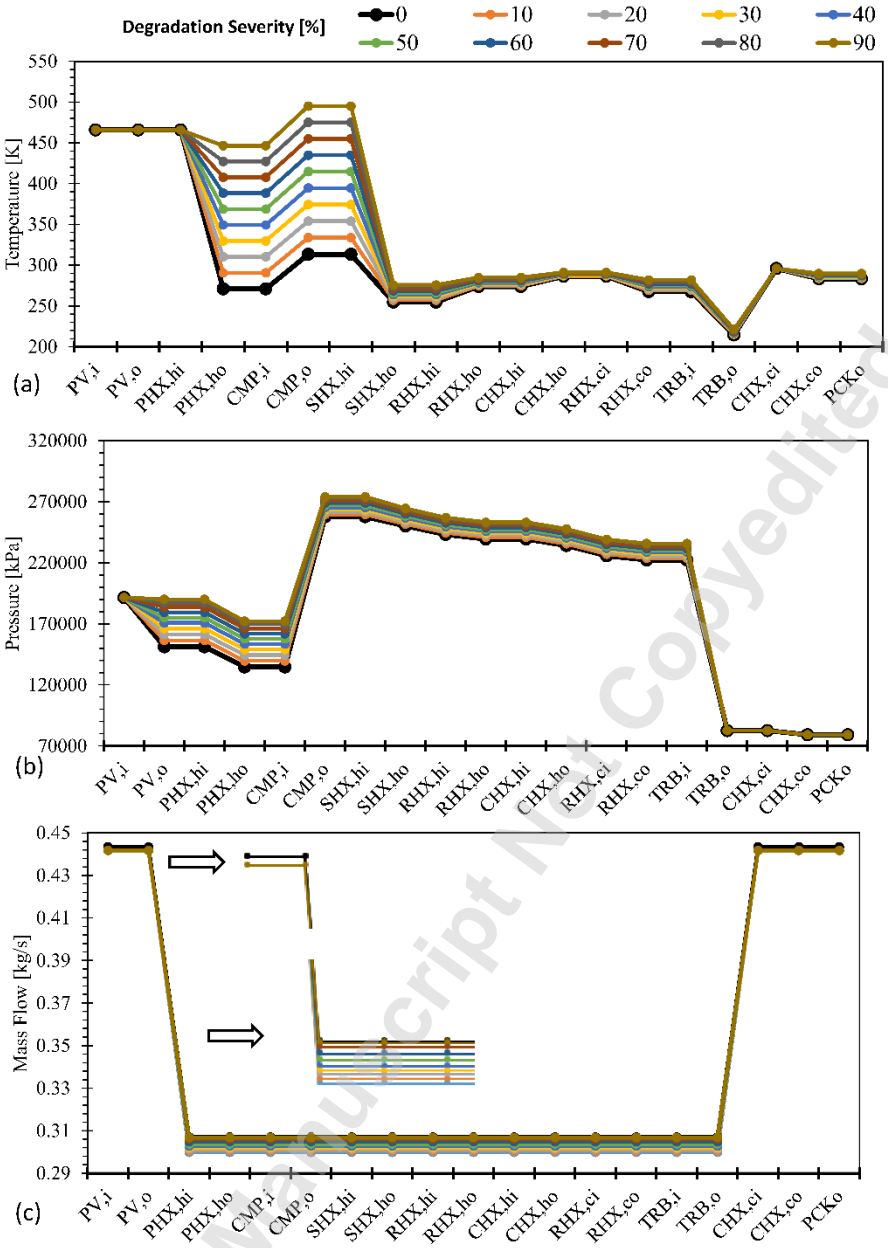


Figure 12: PHX degradation simulation results for RC1.

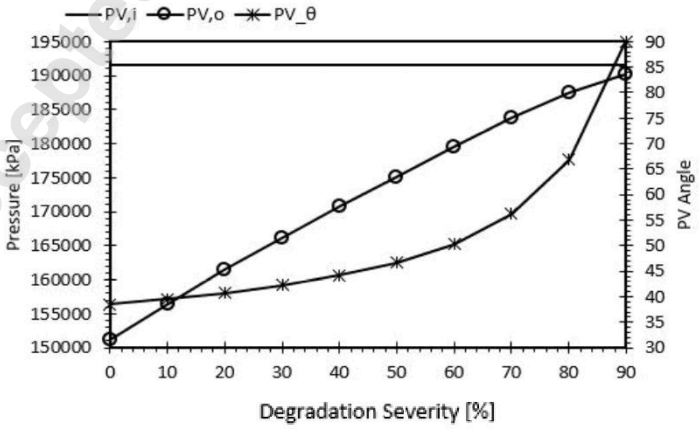


Figure 13: Variation in PVIP, PVOP, and PV angles, PHX degradation simulation results for RC1.

Accepted Manuscript Not Copyedited

Journal of Thermal Science and Engineering Applications. Received September 17, 2021;
Accepted manuscript posted January 25, 2022. doi:10.1115/1.4053740
Copyright © 2022 by ASME

4.1.2 RC2 PHX Degradation

The simulation results for the PACK performance characteristics under PHX degradation are presented in Figure 14 for RC2. It is evident from Figure 14 that the performance characteristics remain similar to RC1, except the mass flow. In terms of the mass flow it can be observed that, relative to the RC1, the mass flow at the PV inlet remains constant for all the degraded cases, despite the presence of back pressure on the PV. The PV is able to maintain the target mass flow against the imposed back pressure caused due to the closure of the TCV. This stems from the fact that even in the worse degraded scenario the PVOP remains substantially lower than the PVIP (Figure 15b), resulting in sufficient pressure drop across the PV to maintain target mass flow. The PV under these conditions is only required to marginally adjust its opening to match the target mass flow as shown in Figure 15c. Based on the results acquired for both RCs, it can be claimed that the proposed PACK control logic in section 3.3 enables the acquisition of accurate engineering design and physics of the PACK both under healthy and degraded functional scenarios. The model can now be further used to assess malfunction in PV and TCV.

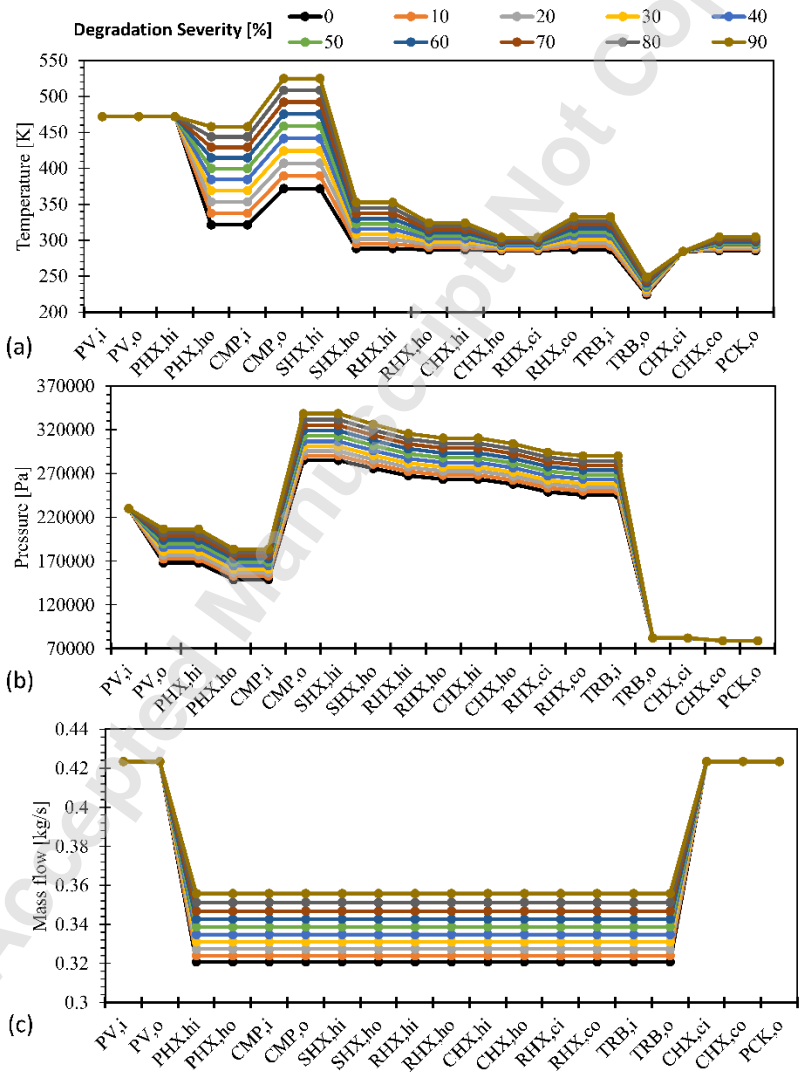


Figure 14: PHX degradation simulation results for RC2.

Accepted Manuscript Not Copyedited

Journal of Thermal Science and Engineering Applications. Received September 17, 2021;
Accepted manuscript posted January 25, 2022. doi:10.1115/1.4053740
Copyright © 2022 by ASME

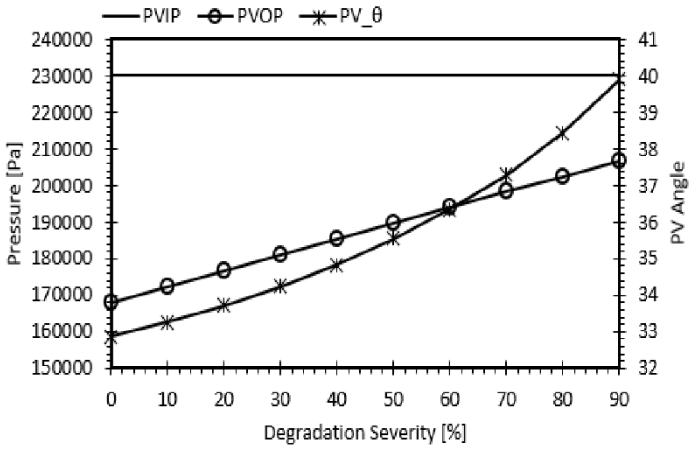


Figure 15: Variation in PVIP, PVOP, and PV angles, PHX degradation simulation results for RC2.

4.2 Malfunction of Control Valves

This section presents the results acquired based on the simulation of PV and TCV malfunction for RC1. The malfunction for PV and TCV is simulated by overshooting or undershooting the valve angle from the healthy baseline valve angle presented in Table 5. The impact of PV and TCV valve malfunction on the performance characteristics of the PACK is presented at various severities.

4.2.1 PV Malfunction

Table 5 presents the percentage overshoot and undershoot of the PV relative to the baseline healthy valve angle. The simulations are conducted by changing the PV controller saturation limit to the corresponding values of the overshoot/undershoot, while making no changes to the TCV controller. The acquired results in terms of temperature, pressure and mass flow are presented in Figure 16. As shown in Figure 16(c), the overshoot of the PV results in increased mass flow through the PV. This is to be expected as the PV opening increases, reducing the pressure drop across the PV and allowing more mass flow. The increased mass flow through the core of the PACK increases the expansion through the turbine, resulting in colder turbine outlet temperature relative to the baseline, as shown in Figure 16(a). Under these conditions, the TCV is required to increase the supply of hot mass flow in order to match the target temperature. As tabulated in Table 4, the TCV valve opening increases with increase in the severity of the overshoot.

Interestingly, as highlighted in Figure 16(a), the PHX outlet temperature increases as a result of the PV overshoot. This can be attributed to the fact that, as more hot mass flow is fed through the hot side of the PHX, the RAM mass flow on the PHX cold side remains unchanged. Therefore, the heat transfer across the PHX drops, which results in the increased PHX outlet temperature.

With regards to the undershoot of the PV, exactly the opposite response in the PACK performance characteristics can be observed. The closing of the PV results in reduced overall mass flow relative to the healthy case, this reduces the mass flow through the core, which reduces the expansion through the turbine, resulting in warmer turbine outlet temperature relative to the healthy case. The TCV must close in order to reduce the hot mass flow to match target temperature.

Table 5: TCV variation with PV malfunction.

Accepted Manuscript Not Copyedited

Journal of Thermal Science and Engineering Applications. Received September 17, 2021;
Accepted manuscript posted January 25, 2022. doi:10.1115/1.4053740
Copyright © 2022 by ASME

% PV Overshoot/undershoot	PV Angle [º[	TCV Angle [º[
40	56.0	22.5
30	52.0	22.2
20	48.0	21.9
Healthy	40.0	20.4
-20	32.0	18.9
-30	28.0	17.6
-40	24.0	15.7

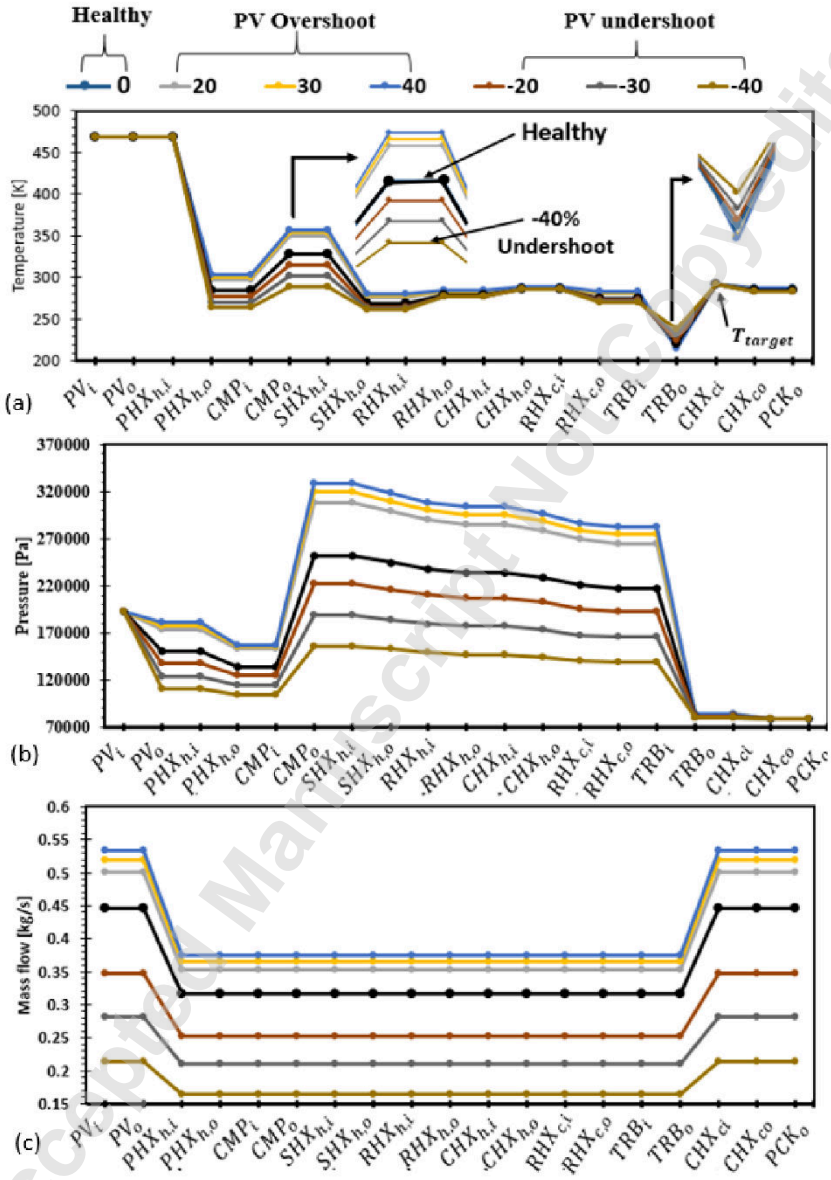


Figure 16: Simulation results for PACK performance characteristics under PV malfunction.

Accepted Manuscript Not Copyedited

Journal of Thermal Science and Engineering Applications. Received September 17, 2021;
Accepted manuscript posted January 25, 2022. doi:10.1115/1.4053740
Copyright © 2022 by ASME

4.2.2 TCV Malfunction

Table 6 presents the percentage overshoot and undershoot of the TCV, relative to the baseline healthy valve angle of RC1. The simulations are conducted by changing the TCV controller saturation limit to the corresponding value of the overshoot/undershoot, while making no changes to the PV controller. The acquired results in terms of temperature, pressure and mass flow are presented in Figure 17. In the case of overshoot, the increase in TCV opening relative to the healthy case will alleviate the back pressure from the PV, which will increase the pressure drop across it, resulting in reduced PACK inlet mass flow. In this scenario, relative to baseline the core mass flow drops which consequently results in warmer turbine outlet temperature, as the expansion through the turbine reduces compared to baseline. With the TCV being stuck at increased opening angle, the hot mass flow through the TCV increases, as a result the temperature at the merge outlet overshoots the target temperature. It can be said that, in a scenario where the TCV overshoot severity increases well beyond 30%, the PACK outlet overheat thermal switch (see, section 2.1, Table 1) which has an activation threshold of (121℃/394 K) will be activated, and the PACK control system will shut down the PV to prevent overheating. Lastly, due to the drop in core mass flow, while cold mass flow through the RAM remains unchanged, resulting in improved heat transfer across the PHX relative to healthy case.

In terms of the TCV undershoot, which represents the closing of the TCV relative to the healthy case, due to the closing of the TCV, the back pressure on the PV increases, reducing pressure drop across PV, against this back pressure, PV opening increases, and so does the mass flow through the core. Due to increased core mass flow, and turbine expansion, colder turbine outlet temperature results when compared to the healthy case. As the TCV is undershooting and is stuck, this leads to the lack of sufficient hot mass flow supply through the TCV, and as a consequence the merge outlet temperature undershoots the target temperature. For a fixed cold RAM mass flow, the increased core mass flow also has a detrimental impact on heat transfer through the PHX.

Table 6: Variation in PACK performance characteristics parameters under TCV malfunction.

% TCV Overshoot/undershoot	PV Angle [º[	TCV Angle [º[
30	36.9	26.4
20	37.8	24.4
10	39.0	22.4
Healthy	40.0	20.4
-10	43.6	18.4
-20	47.1	16.4
-30	50.2	14.4

Accepted Manuscript Not Copyedited

Journal of Thermal Science and Engineering Applications. Received September 17, 2021;
Accepted manuscript posted January 25, 2022. doi:10.1115/1.4053740
Copyright © 2022 by ASME

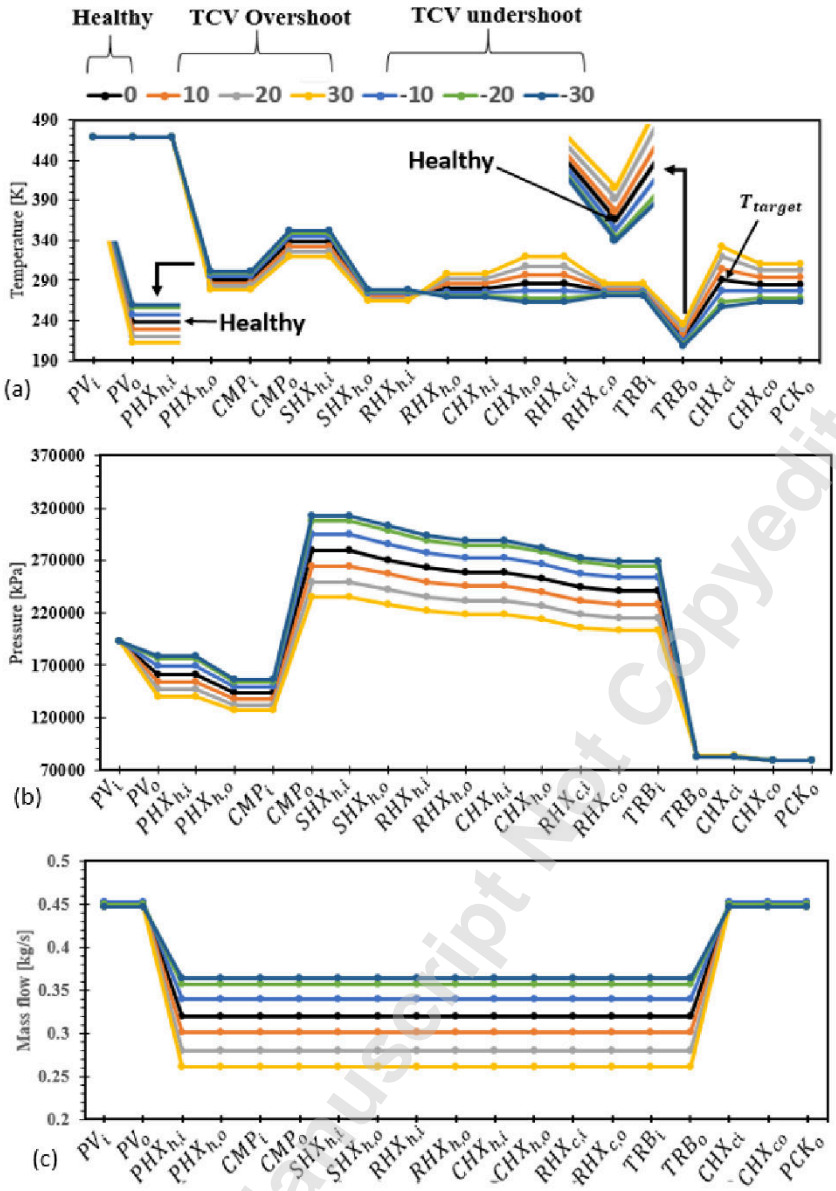


Figure 17: Simulation results for PACK performance characteristics under TCV malfunction at various severities.

5 Conclusions

In this paper, the overall control system of the B737-400 PACK has been investigated in order to support the implementation of an accurate simulation model for fault diagnostics. The PACK control system elements, i.e. mass flow and temperature control valves, RAM flow control, and overheat protection control system, are discussed and their operation is verified against the actual data acquired from the Cranfield B737-400 aircraft.

Based on the assessment and understanding of the PACK in-situ control system improvements in the previously employed PACK control system are proposed for accurate fault simulation. An integral controller for the control of the TCV and PV are proposed, and implemented to simulate PHX degradation at various severity levels at two reference aircraft cruise conditions. Based on the acquired results it was verified that the proposed control logic accurately captures the engineering and physics of the PACK under both health and degraded functional scenarios. Finally, the simulations were further exercised to assess the malfunction

Accepted Manuscript Not Copyedited

Journal of Thermal Science and Engineering Applications. Received September 17, 2021;
Accepted manuscript posted January 25, 2022. doi:10.1115/1.4053740
Copyright © 2022 by ASME

in the TCV and PV at various severities. The impact of TCV and PV malfunction on the PACK performance characteristics in terms of temperature, pressure and mass flow was presented and discussed.

The B737-400 PACK simulation proposed in this paper enables the accurate fault simulation of the sub-systems at various degradation severities, which serves as a foundation for formulating accurate diagnostics. The developed model application will be further extended to produce a robust diagnostics solution for an aircraft PACK.

6 Acknowledgments

The Boeing Company, as part of their collaboration with Cranfield University's IVHM Centre, funded this work; the authors would like to thank them for their support of this project. The authors would also like to thank Mr. Cengiz Turkoglu (Senior Lecturer at the Safety Engineering Centre, Cranfield University) for providing his expert support to aid the aircraft experimentation and data collection.

7 References

1. Jennions, I., Ali, F., 2021, "Assessment of Heat Exchanger Degradation in a Boeing 737-800 Environmental Control System," ASME, J Therm Sci Eng Appl, 13(6), pp. 155 – 168.
2. Esperon, M., Jennions, I., Escobar, I., Hanov, N., 2020, "Simulating faults in a Boeing 737-200 environmental control system using a thermodynamic model". International Journal of Prognostics and Health Management, 10(2), pp. 540 – 552.
3. Esperon, M., Philip, J., Jennions, I., 2013, "A review of Integrated Vehicle Health Management tools for legacy platforms: Challenges and opportunities"., Journal of Progress in Aerospace Sciences, 56, pp.19-34.
4. Ezhilarasu, C., Skaf, S., Jennions, I., 2021, "A Generalised Methodology for the Diagnosis of Aircraft Systems"., IEEE Access, 9, pp. 11437-11454.
5. Ezhilarasu, C., Skaf, S., Jennions, J., 2019, "Application of Reasoning to Aerospace Integrated Vehicle Health Management (IVHM): Challenges and Opportunities"., Progress in Aerospace Sciences, 105, pp. 60-73.
6. Ezhilarasu, C., and Jennions, I., 2020, "A system-level failure propagation detectability using ANFIS for an aircraft electrical power system", Journal of Applied Sciences,10(8), 2854.
7. Jennions, I., Ali, F., Esperon, M., Escobar, I., 2020, "Simulation of an aircraft environmental control system"., Appl. Thermal. Eng. 172, pp. 1125-1139.
8. Shafayat, C., Ali, F., Jennions, I., 2019, "A Methodology for the Experimental Validation of an Aircraft ECS Digital Twin Targeting System Level Diagnostic"., Proceedings of annual conference of the prognostics and health management society, 11th PHM Conference, Scottsdale, AZ, USA, September 21-26.
9. Boeing 737-300/400/500 Aircraft Maintenance Manual, D6-37580.

Accepted Manuscript Not Copyedited

Journal of Thermal Science and Engineering Applications. Received September 17, 2021;
Accepted manuscript posted January 25, 2022. doi:10.1115/1.4053740
Copyright © 2022 by ASME

10. Glen I., NSW Australia 2016", Skybrary, B737 en-route, last edited on 26 March 2016. B737 en-route, Glen Innes NSW Australia, 2007 | SKYbrary Aviation Safety.

Accepted Manuscript Not Copyedited



https://dspace.org/

Boeing 737-400 passenger air conditioner control system model for accurate fault simulation

Chowdhury, Shafayat H.; Ali, Fakhre; Jennions, Ian K.

2022-03-08
American Society of Mechanical Engineers (ASME)
https://doi.org/10.1115/1.4053740
Chowdhury S, Fakhre A, Jennions IK. (2022) Boeing 737-400 passenger air conditioner control system model for accurate fault simulation. Journal of Thermal Science and Engineering Applications, Volume 14, Issue 9, September 2022, Paper number TSEA-21-1530

Downloaded from a DSpace repository. https://dspace.org/